COURRIER DU SAVOIR – N°24, Septembre 2017, pp.93-100

SUBMICRON SIZED SINTERED ODS STEELS PREPARED BY HIGH EFFICIENT ATTRITION MILLING AND SPARK PLASMA SINTERING

LES ACIERS ODS FRITTES DE TAILLE SUBMICRONIQUE PREPARES PAR BROYAGE ET PAR FRITTAGE PAR ETINCELLE

H. RACHID BEN ZINE[1,2], A. HORVATH[2], K. BALAZSI[2], C. BALAZSI[2]

[1]Doctoral School on Materials Sciences and Technologies, Óbuda University, Bécsi út 96/B, 1034 Budapest, Hungary
[2]Hungarian Academy of Sciences, Centre for Energy Research, Konkoly-Thege M. str. 29-33, 1121 Budapest, Hungary

ABSTRACT

This paper summarizes recent results for preparation, structural and mechanical investigation of oxide dispersed strengthened steel (ODS). Three commercial steel powders, two austenitic steel and one martensitic powders have been used as starting materials. One of the austenitic powders was used for morphological study during wet milling. The high efficient attrition mills are on the basis of this work assuring grains with nanostructure. The morphological changes during milling steps have been described. It was demonstrated that 4 hours milling in wet atmosphere are enough to realize steel powders with submicron dimensions. An efficient dispersion of nanosized oxides in ODS steels was achieved by employing high efficiency attrition milling. A combined wet and dry milling process of fine ceramic and steel particles has been proposed. Spark Plasma Sintering (SPS) was applied to realize submicron grained steel compacts. Grains with 100 nm mean size have been observed by scanning electron microscopy (SEM) in sintered austenitic ODS. In comparison, the sintered martensitic dry and combined milled ODS microstructure consisted of grain sizes with 100-300 nm in each case.

KEYWORDS: ODS Steel, Spark Plasma Sintering (SPS), attrition milling, Nano-oxides, structural and mechanical investigation

RESUME

Cet article résume des résultats récents relatifs à l'élaboration et la caractérisation structurale et mécanique d'un acier renforcé à l'oxyde (nuance appelée souvent ROD/ODS). Trois poudres commerciales d'acier, deux poudres austénitiques et une poudre martensitique ont été utilisées comme matières d'étude. Une des poudres austénitiques a été utilisée pour l'étude morphologique lors du broyage humide. Le broyage à haute efficacité est sur la base de ce travail assurant l'obtention de grains nanostructurés. Les modifications morphologiques au cours des étapes de broyage ont été bien décrites. Il a été démontré que 4 heures de broyage en atmosphère humide sont suffisantes pour réaliser des poudres d'acier de dimensions submicroniques. Une dispersion efficace des nano-oxydes dans les aciers ROD/ODS a été obtenue en utilisant un broyage spécifique. On a proposé un procédé de broyage humide et sec combiné à des particules de céramique et d'acier. La méthode de frittage par étincelle (spark plasma sintering (SPS)) a été appliquée pour élaborer des aciers compacts à grains submicroniques. Des grains ayant une taille moyenne de 100 nm ont été observés par microscopie électronique à balayage (MEB) dans les aciers ROD/ODS austénitiques frittées. En comparaison, la microstructure de l'acier ROD/ODS martensitique frittée a donné des grains de tailles de 100 à 300 nm dans les deux cas de broyage sec et de broyage combiné (humide et sec).

MOTS CLES: Acier ODS, frittage par étincelle (SPS), broyage, Nano-oxydes, étude structurale et mécanique.

1 INTRODUCTION

Oxide-dispersion strengthened steels (ODS) have attracted attention for advanced nuclear applications such as fast and fusion reactors as other commercially available materials can hardly be used in harsh environments at high neutron doses and elevated temperatures [1]. Many countries such as Japan, Europe, and the United States have developed and investigated this material for nuclear fission and fusion applications [2,3]. The production of ODS involves many technological processes, such as mechanical alloying, degassing, canning, hot extrusion, and heat treatments. Powder metallurgy processes are applied to finely disperse these small oxide particles in the matrix, because oxide particles aggregate together and coarsen during conventional casting processes [4]. Nanostructured ferritic, martensitic or austenitic ODS alloys are ideal candidates for high temperature applications such as high temperature heat exchangers or nuclear power plants [5–9]. Novel designs for future generation fusion reactors have demanding requirements for the structural materials. A new class of ODS materials which are currently being developed have a high chance of meeting these requirements [10]. The application of ODS steels as functional or structural application strongly depends on the availability of large batches of materials. Since no commercial ODS-alloys are available at the moment, investigations on large scale batches are crucial for future applications [11]. In order to better exploit the potential advantages of ODS steels, such as improved creep strength and damage tolerance in comparison to the non-ODS high-chromium steels along with excellent oxidation resistance, a broader scientific and technical background is required [12, 13]. In previous works model ODS alloys (Fe–0.3Y_2O_3, Fe–0.2Ti–0.3Y_2O_3 and Fe–14Cr–0.2Ti–0.3Y_2O_3) were prepared by ball milling and then hot extrusion to study the effect of Ti and Cr on the size, distribution, crystal structure and composition of the nano-oxide particles. All alloys were characterized by high resolution transmission electron microscopy (HRTEM), atom probe tomography (APT) and synchrotron-X-ray diffraction (S-XRD) to determine the distribution, structure and composition of the oxide nanoparticles samples. The median particle sizes were 9.6 nm, 7.7 nm and 3.7 nm for the Fe–Y2O3, Fe–Ti–Y_2O_3 and Fe–Cr–Ti–Y_2O_3 alloys, respectively, so the presence of Ti resulted in a significant reduction in oxide particle diameter and the addition of Cr gave a further reduction in size [14]. In an other example Fe-25 wt%Y_2O_3 composite powders have been fabricated by mechanical milling (MM) Fe powders of 100 μm in diameter and Y2O3 nanoparticles in an argon atmosphere for the milling periods of 4, 8, 12, 24, 36, and 48h, respectively. The experimental results showed that the mean particle size and crystalline size of MM powders decreased with the milling time increasing. All the elements distributed homogenously inside the powders after 48h of MM. The lattice constant of the matrix α-Fe kept constant with the milling time, and no solid solution took place during MM process [15]. Novel sintering techniques have been used for preparation of ODS. A Fe–14Cr–0.4Ti + 0.25 Y_2O_3 alloy was fabricated by mechanical alloying and subsequently consolidated by spark plasma sintering (SPS). The densification of these alloys significantly improved with an increase in the sintering temperature. Scanning electron microscopy and electron backscatter diffraction revealed that SPS-sintered at 1150 °C under 50 MPa for 5 min had a high density (99.6%), a random grain orientation and a bimodal grain size distribution (<500 nm and 1–20 μm) [16].

This paper presents recent results for the preparation, structural and mechanical investigation of oxide dispersed strengthened steel (ODS) by employing high efficiency attrition milling and spark plasma sintering. Nanosized yttria dispersed martensitic and austenitic steel compacts with nanostructure have been realized. A combined wet and dry milling process of fine ceramic and steel particles is proposed to achieve the efficient oxide dispersion. Structural, morphological and mechanical properties of nanostructured ODS steel powders and compacts are presented.

2 EXPERIMENTAL

2.1 Starting material

Commercial “Höganas 316 L” austenitic stainless steel (17Cr12Ni2.3Mo0.1Mn0.9Si), austenitic „Metco 41C” (Fe17Cr12Ni2.5Mo2.3Si0.1C, AISI Type 316 stainless steel, water atomized, particle size: -106+45 μm) and martensitic „Metco 42C” (Fe16Cr2Ni0.2C, AISI Type 431 stainless steel, water atomized, -106+45 μm) powders were used for samples preparation. Yttria with mean particle size 700 nm (grade C) has been purchased from Starck GmbH.

2.2 Milling process

Based on our former observations the attritor mill has more advantages to conventional planetary mill [17]. In the wet process, the attritor may work at speeds of agitator rotation high as 3000 rpm in comparison to planetary mill that can have 350 rpm. The delta discs employed in the attritor, as well as the small media 0.1- 1 mm assure a very efficient dispersion of oxides phases in steel powder. The commercial austenitic powder (Hoganas 316L) was milled by attritor for 1, 2, 3, and 4 hours in ethanol (wet milling) by DMQ 07 Union Process, type 01-HD/HDDM. In the other hand an efficient dispersion of nano-oxides (yttria) in ODS steels was achieved by employing the high efficiency attritor milling. A combined wet milling in ethanol and dry milling process of steel powders together with fine ceramic particles is proposed by rotation speed of agitator high as 600 rpm. A high efficiency attritor mill (Union Process, type 01-HD/HDDM) equipped with a stainless steel setup (tank, agitator, grinding media with 3 mm in diameter) working at 600 rpm was employed consecutively for wet (5h) and dry milling (5h).

2.3 Sintering process

For bulk processing, Spark Plasma Sintering (SPS) was used. This technique has a high potential to process „bulk" nanomaterials with good interparticle bonding [17-20]. The external field application is capable of inducing rapid densification and reasonable control of grain growth during the sintering of steels when starting with submicron grained powders. The main difference between SPS and hot pressing (HP) is the simultaneous application of a pulsed current for SPS, which generates electrical discharges [21,22]. SPS has been applied with success to a wide range of metals, ceramics (oxides, nitrides, carbides) and composites [23]. By using this new sintering method, densification of samples without a considerable grain growth process can be achieved within few minutes. A set of composites were sintered by the help of spark plasma sintering, with the system capacity 10 V and 20,000 A from Sojitz Japan, Dr. Sinter-SPS-7.40MK-VII installed in Istanbul Technical University. The sintering was performed in vacuum, 50 MPa mechanical pressure, temperature 900-980°C and 5 minutes dwelling time were applied. Circular samples of 50 mm in diameter and 5 mm in thickness have been produced. These samples have been cut by diamond wheels to bars with rectangular geometry (4x5x30 mm in dimension).

2.4 Techniques of characterization

Morphology and microstructure of the powder and the fracture surface of sintered steels were studied by scanning electron microscope (Zeiss-SMT LEO 1540 XB and Jeol JSM-25-SIII). Phase analyses were performed on an X-ray diffractometer (Bruker AXS D8) with CuKα radiation. Hardness was determined using a Leitz Miniload2 microscope and micro- Vickers hardness tester by applying two loads 5 and 10 N for 10 seconds. Three points bending strength was determined on an Instron 1112 tensile/loading machine equipped with a data acquisition system. The fractured samples obtained after bending tests were passed to electron microscopy investigations.

3 EXPERIMENTAL RESULTS

3.1 Morphological characterization

Morphological characterization of starting austenitic steel powder was performed by scanning electron microscopy (Figure 1a). Austenitic sample consisted of globular particles. The average size of particles is between 50 – 100 μm. The powder structure after 1 hour milling showed considerable differences to the starting powder. The form of austenitic particles is still globular. Their average size is lower, about 80 μm (Figure 1b). The morphological investigations demonstrated the existence of small grains in few micrometer ranges among globular grains (Figure 1b insert.)

Figure 1c shows the morphology of austenitic sample after 2 hours milling time. The average size of globular particle is about 60 μm. Another hour of intensive high efficient milling decreased the particle size about to 15 – 20 μm. The shape of grains has not changed, but the surfaces of grains show erosion (Figure 1c insert). After 4 hours wet milling, the structure showed drastically change in morphology. The sample consisted of bimodal grains, in one hand a very small austenitic grains with lamellar structure and secondly of few 80 μm size globular particles (Figure 1d). The average size of lamellar particles in one dimension is nanometer range in thickness, whereas their length is few micrometers (Figure 1d).

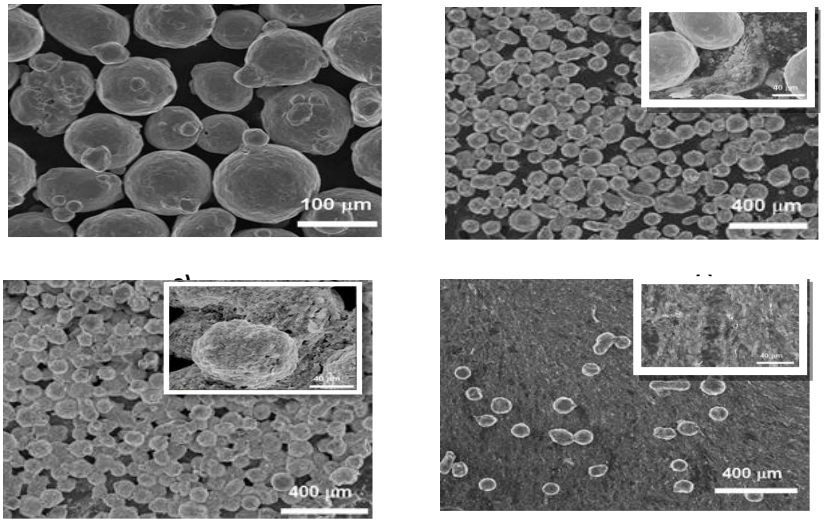

c) *d)*

Figure 01: SEM micrographs of a) starting commercial austenitic powder (Höganäs 316L), b) austenitic powder milled for 1 hour, c) austenitic powder milled for 2 hours, d) austenitic powder milled for 4 hours

The Figure 2a shows schematic draw of powder grain changes and the evolution of grain morphology during milling process.

On Figure 2b we can observe the scanning electron microscopy images of final powder grain shape after milling.

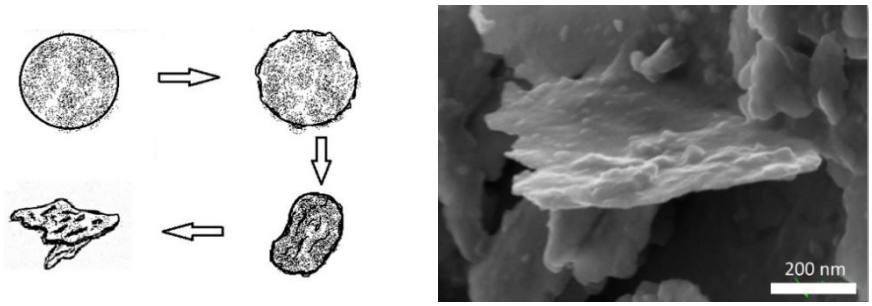

a) *b)*

Figure 01: . a) schematic view of changes of powder grain morphology; the shape transformation process. b): final powder grain shape after milling

4 AUSTENITIC ODS STEEL

SEM investigations of the starting austenitic powder (Metco 41C) and milled powder with a 1% Y_2O_3 addition are shown in Figure 3. The average grain size of the starting powder is about 100 µm (Figure 3a). The structure of powders is considerably changed after this intensive milling as shown in Figure 3b. The metal grain size of austenitic ODS powder is around 2 µm on average. However, these grains are stacked to 5 and aggregates (Figure 3c). Globular and lamellar shaped grains may be also observed. SEM images of austenitic ODS samples prepared by SPS are presented in Figure 3d. From this investigation is shown the homogenous fracture surface of a sintered "bulk" sample and steel grains with 100 nm mean size may be found.

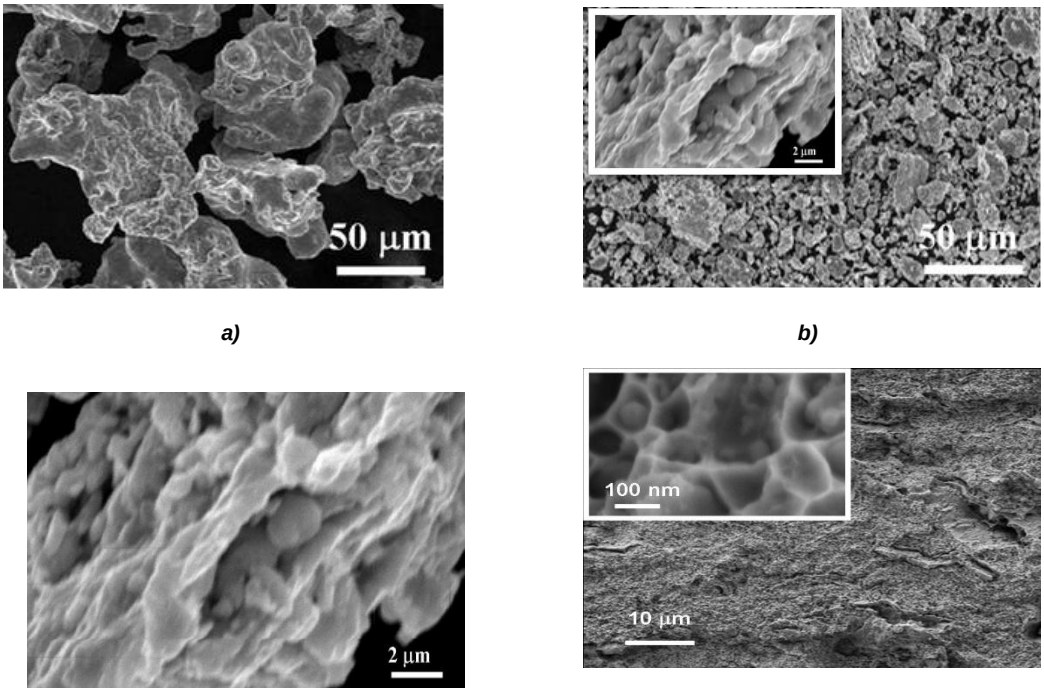

a) *b)*

c) *d)*

Figure 02: SEM Images ; a) starting austenitic powder (Metco 41C), b) austenitic powder with 1% Y_2O_3 prepared by combined milling, c) high magnitude of Figure 1b, d) austenitic milled powder with 1% Y_2O_3 after SPS process (Inside – high resolution image of sintered nano-structure)

The aim of 1 wt.% Yttria addition to the starting powder is to achieve improvements in mechanical properties (strength, creep) at a high temperature (higher than 300 °C).

Phase analyses performed by X-ray measurements are shown in Figure 4. The main lines of cubic Cr0.19Fe0.7Ni0.11 phase (JCPDFWIN 33-0397) and cubic FeNi (JCPDFWIN 03-1209) have been assigned. In the case of commercial austenitic powder (Metco 41C), where the mean grain size was 100 microns, the CrFeNi phase is dominant (2θ = 43.55°, 50.75° and 74.6°). However, the FeNi phase is also present in the powder structure (2θ = 44.5°, 64.2° and 82.1°). The XRD analyses show the structural changes of powder during milling and the following sintering steps (Figure 4). The dominant CrFeNi phase in commercial powder can hardly be observed after milling, but the FeNi main lines became stronger.

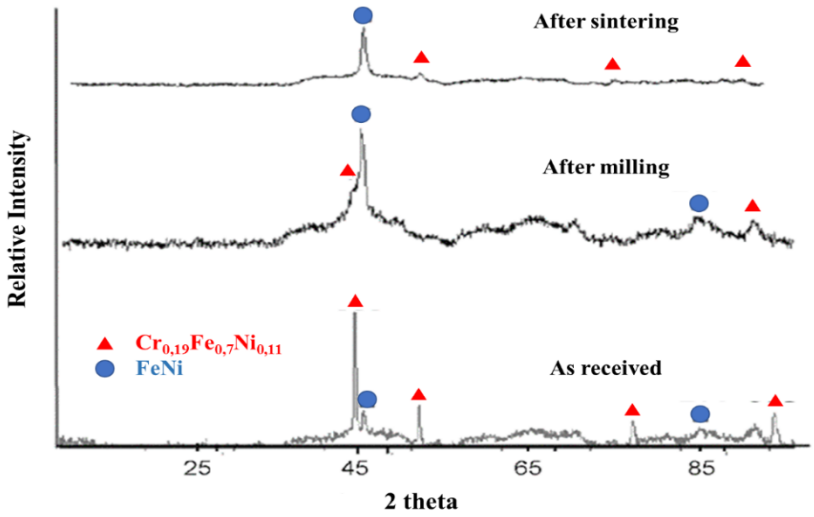

Figure 03: XRD measurement of austenitic powders before, after milling and after sintering

5 MARTENSITIC ODS STEEL

The SEM study of martensitic powders (Metco 42C) is shown in Figure 5. The martensitic ODS powder grain size (Figure 5b) is considerably lowered compared to the initial grain size of the starting powder (Figure 5a). The average grain size is 1-2 microns, but the same sticking tendency is revealed as in the case of austenitic ODS powder. Because of this, the mean secondary grain size can reach 5-10 microns with non-regular morphology, as is shown in Figure 5c. Fracture surfaces of martensitic sintered ODS samples are presented in Figure 5d. The "bulk" ODS steel with a homogenous surface consists of steel grains of 100-300 nm in size.

In the starting martensitic powder the cubic FeCr phase (2θ = 44.7°, 65.4° and 82.3°) (JCPDFWIN 34-0396) is dominant (Figure 6). Minor CrFeNi phase (JCPDFWIN 33-0397) is also present. The average grain size is decreasing without phase change during milling. With the correlation of SEM investigations, the broadening of the FeCr peaks may be related to a decrease of grain size during sintering. The location, dispersion and evolution of yttria in steel matrix is of particular interest in ODS research [18]. In this case, the lines of Y2O3 (JCPDFWIN 82-2415) expected at 2θ = 29.15°, 33.79°, 48.53° and 57.62° could not be observed on the XRD diffractograms.

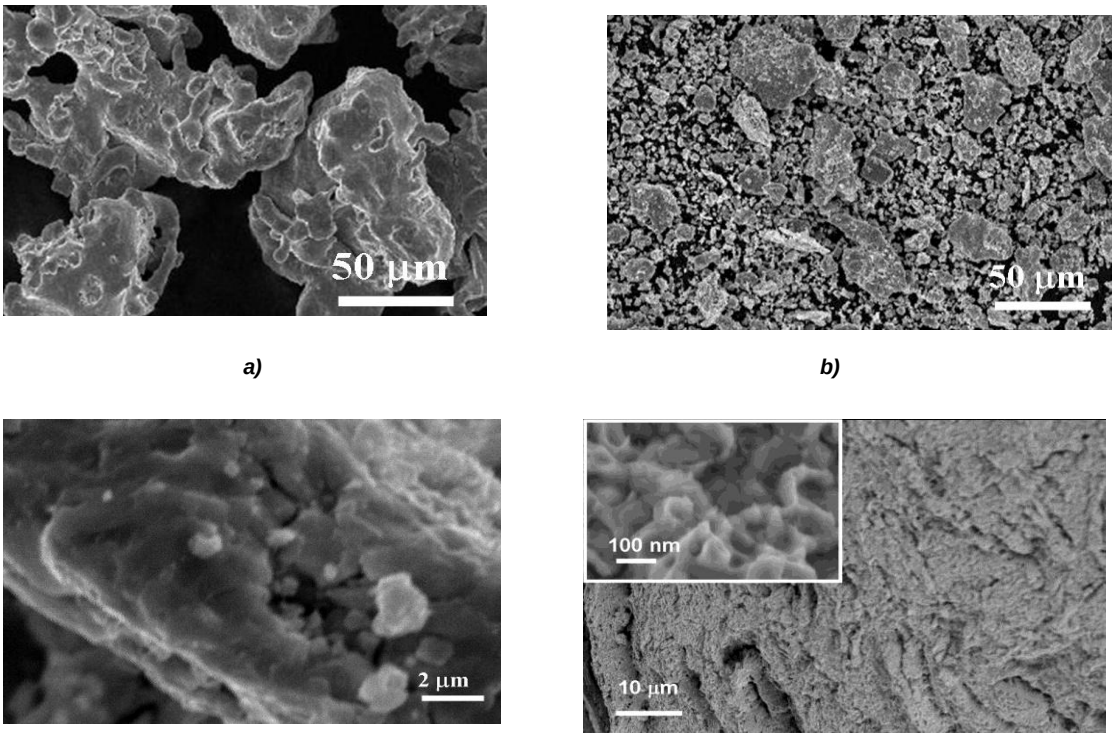

Figure 04: SEM Images; a) starting martensitic powder (Metco 42C), b) martensitic powder with 1% Y_2O_3 prepared by combined milling, c) high magnitude of Figure 4b, d) martensitic milled powder with 1% Y_2O_3 after SPS process (Insert – high resolution image of sintered submicron-structure)

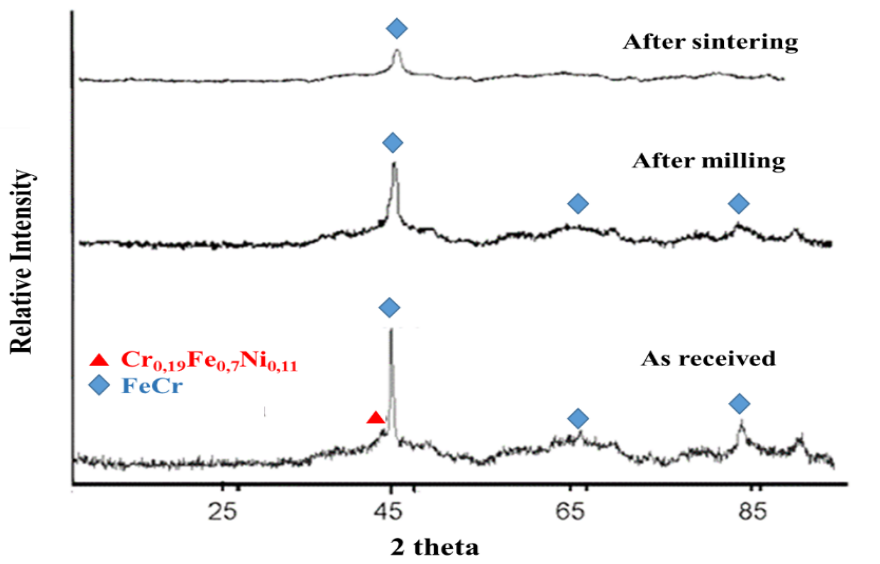

Figure 05: XRD measurement of martensitic powders before, after milling and after sintering

6 MECHANICAL PROPERTIES

The tensile strength measurements details are presented in Table 1. Martensitic ODS samples showed higher values than austenitic ODS samples.

Table 01: Tensile strength, bending strength and modulus of elasticity values of ODS samples

	Martensitic ODS + 1 wt%Y_2O_3	**Austenitic ODS + 1wt% Y_2O_3**
Rm, MPa, 20 °C	832,1±45	638,95±32
Rm, MPa, 500 °C	580,1±25	415,4±21
Bending strength, MPa	1806,7±82	1210,8±60
$R_{0,002,}$ MPa	29,68±5	24,97±7
Young modulus, GPa	95,2±6	80,9±8

The hardness of sintered ODS was measured with 5 and 10 N load. From these measurements, the Vickers hardness of martensitic ODS with 1% Y_2O_3 addition is higher [HV (5 N) ~ 735 ± 29 and HV (10 N) ~ 849 ± 43] than the austenitic ODS with 1% Y2O3 higher [HV (5 N) ~ 415 ± 18 and HV (10 N) ~ 516 ± 48].

7 CONCLUSIONS

Three commercial steel powders, two austenitic steel and one martensitic powders have been used as starting materials. One of the austenitic powders was used for morphological study during wet milling. The high efficient attrition mills are on the basis of this work assuring grains with nanostructure. It was demonstrated that 4 hours milling in wet atmosphere are enough to realize steel powders with submicron dimensions. The morphology and structure of powders is considerably changed after high efficiency attritor milling consisting of a wet and dry process. The grain size of steel powders was reduced from the starting 100 μm to a few microns. The milled grains were stacked to 5-20 μm aggregates presenting a non-regular morphology at the same time. Dense samples showing submicron characteristics have been achieved after sintering at only 900-980 °C for 5 minutes by spark plasma sintering. Grains of steel with 100 nm mean size have been observed by SEM in austenitic and with 100-300 nm in martensitic ODS. The martensitic ODS is twice as hard as the austenitic ODS. The combined milling resulted in hardness and bending strength increases.

ACKNOWLEDGMENTS

This study was supported by grants Stipendium Hungaricum Scholarship from Tempus Public Foundation to Ben Zine Haroune Rachid, MTA EK project “Development of ODS steel preparation by powder technology”. The authors thank to Zsolt. E. Horváth for XRD measurements and Levente Illés for SEM investigations. The authors thank to sintering experiments to Prof. Filiz Cinar Sahin, Istanbul Technical University.

REFERENCES

[1] J.L. Lin et al (2016), “In situ synchrotron tensile investigations on 14YWT, MA957 and 9-Cr ODS alloys”, J. of Nuclear Mat. 471, pp. 289–298.

[2] S. Ukai et al (1999), “Preliminary Tube Manufacturing of Oxide Dispersion Strengthened Ferritic Steels with Recrystallized Structure”, J. Nucl. Sci. Technol., 36, pp. 710-712.

[3] D. K. Mukhopadhyay, F. H. Froes, D. S. Gelles, (1998), “Development of oxide dispersion strengthened ferritic steels for fusion, J Nuclear. Mat., vols. 258–263, pp. 1209-1215.

[4] H. Sakasegawa, M. Tamura, S. Ohtsuka, (2008), “Precipitation behavior of oxide particles in mechanically alloyed powder of oxide-dispersion-strengthened steel”, J. Alloys & Compounds, vol. 452, no. 1, p. 2-6.

[5] S. J. Zinkle, N. M. Ghoniem, (2000), “Operating temperature windows for fusion reactor structural materials”, Fusion Eng. Des., vols. 51–52, pp. 55-71.

[6] [6]- G. R. Odette, M.J. Alinger, B. D. Wirth, (2008), “Recent Developments in Irradiation-Resistant Steels”, Annu. Rev. Mater. Res., vol. 38, pp. 471-503.

[7] Y. Guerin, G. S. Was, S. J. Zinkle, (2009), “Materials challenges for advanced nuclear energy systems” MRS Bull., vol. 34, 2009, p. 10-14.

[8] C. L. Chen, A. Richter, R. Kögler, G. Talut (2011), “Dual beam irradiation of nanostructured FeCrAl oxide dispersion strengthened steel”, J. of Nuclear Mat., 412, Issue 3, pp. 350–358.

[9] Duffy, DM. (2010), Fusion power: a challenge for materials science, Philos. Trans. R. Soc. A, vol. 368, 2010, p. 3315-3328.

[10] R.L. Klueh (2002), “Tensile and creep properties of an oxide dispersion-strengthened ferritic steel”, J. of Nuclear Mat. 307–311, pp. 773–777.

[11] J.Hoffmann et al, (2015), “Microstructural anisotropy of ferritic ODS alloys after different production routes”, Fusion Engineering and Design, 98–99, pp. 1986–1990.

[12] I. Hilger et al, (2016), “Fabrication and characterization of oxide dispersion strengthened (ODS) 14Cr steels consolidated by means of hot

isostatic pressing, hot extrusion and spark plasma sintering" , J. of Nuclear Mat., Vol. 472, pp. 206-214.

[13] T. Chen et al. (2015), Microstructural changes and void swelling of a 12Cr ODS ferritic martensitic alloy after high-dpa self-ion irradiation", J. of Nuclear Mat. 467, pp. 42-49.

[14] A.J. London et al (2015), "Effect of Ti and Cr on dispersion, structure and composition of oxide nano-particles in model ODS alloys", Acta Materialia 97, pp. 223–233.

[15] T. Liu et al (2013), "Structure evolution of Y2O3 nanoparticle/Fe composite during mechanical milling and annealing", Prog. in Natural Sci.: Mat. Int., 23(4), pp. 434–439.

[16] H. Zhang et al (2015), "Processing and microstructure characterisation of oxide dispersion strengthened Fe–14Cr–0.4Ti–0.25Y2O3 ferritic steels fabricated by spark plasma sintering", J. of Nuclear Mat. 464, pp. 61–68.

[17] C. Balázsi, F. Gillemot, M. Horváth, F. Wéber, K. Balázsi, F. C. Sahin, Y. Onüralp, Á. Horváth, (2011), "Preparation and structural investigation of nanostructured oxide dispersed strengthened steels", J. Mat. Science 46:(13) pp. 4598-4605.

[18] M. Palm, J. Preuhs, G. Sauthoff, (2003), "Production scale processing of a new intermetallic NiAl–Ta–Cr alloy for high-temperature application: Part II. Powder metallurgical production of bolts by hot isostatic pressing", J. Mat. Process. Tech. 136, pp. 114-119.

[19] R. Chaim (2007), "Densification mechanisms in spark plasma sintering of nanocrystalline ceramics", Mat. Sci. and Eng.: A, 443, Issues 1–2, pp 25–32.

[20] C. Balázsi et al (2005), "Processing of carbon nanotube reinforced silicon nitride composites by spark plasma sintering", Comp. Sci. and Tech., 65, Issue 5, pp. 727–733.

[21] M. Seifert et al (2015), "Nb(Si,C,N) composite materials densified by spark plasma sintering", J. of the Eur. Ceramic Soc.,35, Issue 12, pp. 3319–3327.

[22] C. Lu et al (2016), "Microstructure of HIPed and SPSed 9Cr-ODS steel and its effect on helium bubble formation", J. of Nuclear Mat., Volume 474, pp. 65–75.

[23] Z. Li et al (2016), "Effect of spark plasma sintering temperature on microstructure and mechanical properties of 14Cr-ODS ferritic steels", Mat. Sci. and Eng.: A, 660, pp. 52–60.